s-Dipentacene: Structure, Spectroscopy, and Temperature- and Pressure-Dependent Photochemistry

Otto Berg,[†] Eric L. Chronister,* Tomihiro Yamashita,[‡] and Gary W. Scott*

Department of Chemistry, University of California at Riverside, Riverside, California 92521

Robert M. Sweet

Biology Department, Brookhaven National Laboratory, Upton, New York 11973

Joseph Calabrese

E.I. DuPont de Nemours & Co., P.O. Box 80228, Wilmington, Delaware 19880-0228

Received: October 14, 1998; In Final Form: December 30, 1998

We report the synthesis, characterization, spectroscopy, and photochemistry of *s*-dipentacene (see Figure 1). The symmetric addition product dimer of pentacene (*s*-dipentacene) is formed upon irradiation of a solution of pentacene. The structure of *s*-dipentacene was determined by X-ray crystallography. The crystals had a space group symmetry of $P\bar{1}$ with two molecules per unit cell. One molecule in the unit cell was accompanied by two dichloromethane molecules of solvation. Photodecomposition of s-dipentacene, dispersed in a poly(methyl methacrylate) (PMMA) host matrix, to pentacene was studied. Spectroscopic evidence shows that this photodecomposition proceeds through a trapped intermediate both at low temperature (∼12 K) and at room temperature under high pressure (13 kbar). This intermediate is assigned as a "broken dimer" of two pentacene molecules trapped in the PMMA host. We previously reported similar results in the photolysis of both dianthracene and ditetracene at low temperatures, but this is the first report of broken dimer formation at room temperature under high pressure.

1. Introduction

The photodimerization of linear polyacenes was first reported in the synthesis of dianthracene from anthracene in 1866.[1] Later, this synthesis was discussed in more detail.[2] However, the molecular structure of dianthracene was not determined until 1955.[3] Several other homodimers of linear polyacenes, including the *syn* and *anti* forms of ditetracene, have also been prepared.[4,5] In addition to these homodimers, mixed dimers and related structural isomers have also been reported.[1−6] One study of the triplet state of pentacene in solution reported observation of a transient dimer of pentacene, but a stable photodimer of pentacene was not prepared under the conditions used in that study.[7] As further noted in that study,[7] an earlier report of the apparent respective photodimerizations of anthracene, tetracene, and pentacene[8] was presumed to be incorrect. The observed products in that even earlier study[8] were most likely to be those of photodecomposition resulting from the short wavelength UV irradiation used in the procedure.

The molecular class of aromatic dimers has drawn particular interest because the reverse photochemical decomposition reaction, which reproduces the two original aromatic monomers, is often efficiently and selectively driven by light. In principle, such a pair[9] of reversible photochemical reactions can serve as the basis of selectively erasable optical devices. However, this possibility raises detailed issues of molecular mobility and intermolecular electronic coupling in the condensed phase host. These dimers can serve as precursors of a pair of closely associated monomers, which, after dissociation, may remain trapped together, diffuse apart, or recombine, depending upon the conditions of the host substrate. Matrix-isolated pairs of molecules that interact strongly in the excited electronic state but that are not chemically bound have been identified spectroscopically as products of the photolysis of dianthracene[10] and ditetracene[11] at low temperature.

Crystal structures of dianthracene[12] and *anti*-ditetracene[13] have been determined. The molecular structures[12,13] of these molecules, as well as those of related photodimers,[14−16] all indicate that the two C−C single bonds joining the two monomer halves of the respective dimer are exceptionally long for such single bonds with lengths on the order of 1.61 to 1.63 Å. Of interest in determining the molecular and crystal structures of *s*-dipentacene is the comparison of these structures with those of related photodimers. The long C−C single bonds between the two halves of such [4+4] photodimerization products produce a weak linkage between these halves. These bonds can be readily broken by the *reverse* photochemical reaction, producing two of the originally linked molecules in close proximity immediately following the reaction.

In a solid host matrix, photodecomposition of these types of photodimers produces two monomers which, at low temperature, may be constrained to a face-to-face "sandwich" configuration that results in a highly red-shifted fluorescence from the trapped monomer pair. This term, "sandwich dimer", is generally used for monomer pairs that are constrained by the matrix to remain in such an energetically unfavorable orientation. This orientation

[†] Present Address: Department of Chemistry, Lensfield Road, Cambridge University, Cambridge, England.

[‡] Present Address: Oji Paper Co., Immermann Strasse 43, 40210 Dusseldorf, Germany.

* To whom correspondence should be addressed.

10.1021/jp984066g CCC: $18.00
Published on Web 03/09/1999

is one that is derived directly from the structure of the chemically bound precursor: face-to-face, parallel, and sterically strained. Ferguson and co-workers have reported several investigations of photochemically produced, sandwich pairs of anthracene.[10] Ferguson has also reviewed the absorption spectroscopy of sandwich dimers and related compounds.[17] In amorphous matrixes, however, the pairs, derived by breaking covalently bound dimers, may have different degrees of local mobility, leading to a distribution of broken pair geometries and interactions strengths, and thus to quite heterogeneously broadened spectra. A more recent review by Bouas-Laurent and Desvergne[18] includes a discussion of the photochemistry of tethered dimers of polyacenes. In these instances, medium rigidity is less important in control of broken pair configurations.

More recently, we have examined the absorption and emission spectroscopy of trapped monomer pairs resulting from the photodecomposition of both *syn*- and *anti*-ditetracene at low temperature in a PMMA host matrix.[11] The spectroscopic manifestations of the interactions between the pair of monomers, even at 12 K, made it clear that these pairs did not retain a sandwich configuration. Rather, we concluded that the two tetracene monomers were free, within some constraints, to adopt a relative configuration in PMMA at 12 K that was at a lower energy than what might be expected of a "sandwich dimer" of tetracene monomers.[11] Furthermore, in the PMMA matrix, there is likely considerable inhomogeneity in the structures of the trapped tetracene monomer pairs.

We have also reported the emission spectra of monomer pairs of 9-alkylanthracene esters following the breaking of their respective photodimers at 12 K in different polymer host matrixes.[19] Host-dependent differences in the evolution of the fluorescence spectrum of these pairs, induced by temperature cycling, were attributed to the increase in monomer pair separation with the increase of the temperature cycle maximum.

We now extend the study of aromatic dimers to the next-larger monomer in the linear polyacene series, pentacene. The present paper reports new results of the synthesis, characterization, structure, and photochemistry of *s*-dipentacene. Evidence is presented for the formation of stable monomer pairs of *s*-dipentacene, not only at low temperature, but also at room temperature under high pressure (~13 kbar). We previously presented preliminary results on the low-temperature photochemistry of *s*-dipentacene[20] and its use as an in situ source of pentacene monomers.[21] We also have published evidence for low-temperature photochemical hole burning of *s*-dipentacene in PMMA at 1.5 K.[22] The present paper presents a more detailed study of the low-temperature and high-pressure photochemistry of this molecule.

We report the spectral characteristics of pentacene monomers produced photochemically from *s*-dipentacene dimers in polymer films. These observations include distorted, red-shifted monomer absorption spectra and the kinetically delayed appearance of a more characteristic monomer spectrum. We discuss whether the observed spectroscopic behavior at low temperature or under high pressure can be accounted for by the trapping of an intermediate form consisting of physically trapped monomer pairs. The evident utility of high pressure as a matrix-isolation method is highlighted. Spectroscopic measurements on trapped monomer pairs of pentacene, resulting from the photodecomposition of *s*-dipentacene, enable us to discuss the structure of this broken photodimer in a PMMA host matrix. Although we have obtained similar results previously at low temperatures for dianthracenes,[19,23] this is the first report of a stable monomer pair under room-temperature conditions at high pressures.

2. Experimental Section

2.1. Synthesis and Sample Preparation. The synthesis of *s*-dipentacene (*s*-P_2) was developed in analogy with the synthesis of the similar molecules of dianthracene and ditetracene for which photochemical syntheses have been published.[1,2,7] The needed reactive collisions between monomers (e.g., one in an excited state and one in its ground state) occur following excitation of dissolved monomers to the S_1 state. Therefore, reaction conditions were chosen to maximize the concentration of excited state monomers: high temperature plus intense, broadband, strongly focused light. In addition, a suitable solvent for the monomer was found, 1-chloronaphthalene, from which the dimer product precipitated directly as a white solid.

Thus, *s*-P_2 was synthesized from 18 mg of pentacene dissolved in ~6 mL of 1-chloronaphthalene. Several freeze−pump−thaw cycles were used to completely degas this reaction mixture. The flask containing the reaction mixture was immersed in a thermostated bath of light mineral oil maintained at 115−125 °C. Green excitation light ($\lambda > 440$ nm) from a 75 W mercury arc lamp was focused on the entrance face of the reaction flask, forming a 5 mm × 2 mm spot on the entrance face. Under the conditions given, the solvent refluxes vigorously, and the *s*-dipentacene product forms as a white, insoluble material on the wall of the reactor above the solution. After 3−5 days most of the undissolved pentacene was depleted, with a corresponding accumulation of product, and the reaction was stopped.

The solid product of the photochemical batch reaction described above was, principally, *s*-dipentacene. To separate it from solvent and from unreacted monomer, the product was filtered and rinsed with methanol to remove chloronaphthalene. Unreacted pentacene was removed by rinsing with dichloromethane. Other impurities and reaction byproducts, such as asymmetric dimers and pentacene oxidation products were removed by rinsing with ethyl ether. Repetition of these rinses produced a higher purity *s*-dipentacene product.

Oxidation of *s*-P_2 occurred slowly when samples were exposed to air even in the dark. The resulting brownish colored product contributed a broad featureless base line to the absorption spectrum with increasing intensity to shorter wavelengths. Oxidation processes were further accelerated in the presence of light. Samples stored in a sealed vessel in the dark were found to be more stable. *s*-P_2-doped PMMA samples were less susceptible to oxidation, but photooxidation was still observed when these samples were exposed to air and light. As with pure *s*-P_2, the *s*-P_2-doped PMMA samples were quite stable, even for years, when stored in a sealed container in the dark.

High molecular weight poly(methyl methacrylate), PMMA, (Aldrich, M. W. ≅ 30000) was used as the host material for photodecomposition experiments. The PMMA was purified by dissolution in dichloromethane, precipitation with methanol, and repetition of this procedure three times. Subsequently, the PMMA was washed with methanol for 11 days in a Soxlet extractor.

s-Dipentacene, 1.2 mg, and 0.40 g of PMMA, corresponding to a final *s*-P_2 concentration of 0.005 M in PMMA, were codissolved in 3 mL of dichloromethane. Blended films of *s*-P_2 in PMMA were cast on a glass plate by slow solvent evaporation in the dark at room temperature. The typical thickness of resulting films was 0.4 mm, and the absorbance due to the dissolved *s*-P_2 was ~0.5 at the naphthalenic peak.

Macroscopic crystals were grown by dissolving purified *s*-dipentacene in CH_2Cl_2 and allowing the solvent to evaporate over a period of approximately 3 days at room temperature.

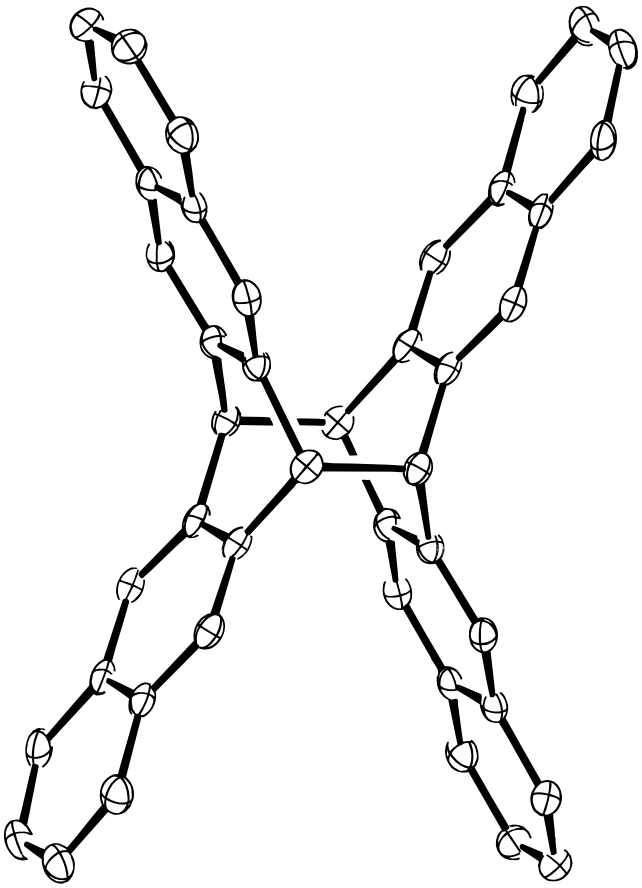

Figure 1. Molecular structure of *s*-dipentacene.

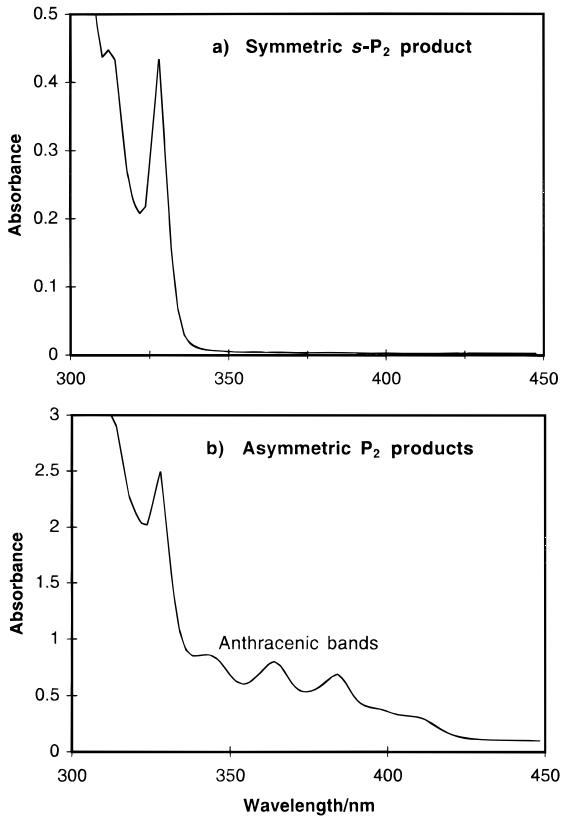

Figure 2. (a) Absorption spectrum of synthesized *s*-P_2 in dichloromethane. (b) Absorption spectrum of a synthesized product mixture which includes asymmetric P_2 products. The additional absorption features not present in (a) correlate with known vibronic features in the anthracene absorption spectrum.

This procedure resulted in needle-shaped crystals with flattened, parallel faces. The crystals appeared clear under a microscope, either colorless or amber-tinted depending on the batch. The largest of these measured approximately 0.2 mm × 0.5 mm × 3 mm, but smaller ones were selected for X-ray crystallographic analysis.

Separation and identification of *s*-P_2 isomers were done as described below. Conceptually, photodimerization of pentacene from solution may produce both symmetric (D_{2h}) and asymmetric dimers of lower symmetry. The latter give UV absorption spectra characteristic of anthracene chromophores (Figure 2b). Only the *s*-P_2 isomer produces exclusively naphthalenic absorption (Figure 2a). The mass spectrum of the symmetric product is consistent with a P_2 isomer.

Three assays were used to assess the synthesis of dipentacene. (1) The near UV lines from a low-pressure mercury lamp were useful for observing the fluorescence of different species. Both solid and dissolved *s*-dipentacene gave a blue emission under this irradiation. Pentacene, solvent, and other impurities yielded other colors or no visible emission under these conditions. (2) Photolysis of *s*-P_2 dimers yielded pentacene monomers. Under UV excitation, the emission from an *s*-dipentacene crystal changes from blue to red, over the course of 30 min under the low-pressure mercury lamp irradiation. The color of the *s*-P_2 crystals also changes from clear/white to pink as pentacene is produced, as observed under a microscope. (3) Reference spectra for 1-chloronaphthalene, naphthalene, anthracene, and benzene in dichloromethane were used to assign the absorption features of the product species. The absorption peak at 328 nm is attributed to the naphthalenic resonance of *s*-dipentacene, as shown in Figure 2a. The vibronic progression, observed in the range 340−390 nm, is similar to that of anthracene, indicating some formation of one or more of the lower symmetry dimer products, as shown in Figure 2b. The absorption cross-section of the *s*-P_2 product, on a weight basis, dispersed in PMMA, was approximately 9000 $cm^2\ g^{-1}$ at the peak of the naphthalenic resonance.

2.2 Spectroscopic Methods. Absorption spectra of the products of *s*-dipentacene/PMMA photolysis were obtained using a Hewlett-Packard diode array spectrophotometer (HP 8451A) with 2 nm resolution. Absorption spectra of *s*-P_2/PMMA films in a high-pressure diamond anvil cell were obtained using a tungsten arc source and a scanning monochromator (SPEX 1402) with 0.1-nm resolution.

Emission spectra of the thin films of *s*-P_2 in PMMA were obtained with a spectrofluorimeter (SPEX Fluorolog 212) equipped with a 450 W Xe lamp source and excitation and emission double monochromators, each with 1.8 nm/mm linear dispersion. Excitation light intensity was monitored with a quantum counter, and fluorescence intensities were measured with a cooled photomultiplier tube (Hamamatsu, R928) used in the photon counting mode. Emission spectra taken in the diamond anvil cell were obtained using an Nd:YAG-laser-pumped dye laser to excite at various visible wavelengths, and the emission spectra were dispersed with the SPEX 1402 monochromator.

Fluorescence spectra of *s*-P_2 and its photodecomposition products were usually taken while the *s*-P_2/PMMA film was held at 12 K. In these experiments, the sample film was sandwiched between two sapphire disks, placed in a copper holder and mechanically attached to the cold stage of a closed-cycle He refrigerator (Air Products, Displex 202E). In these experiments, the temperature was monitored with a gold−iron/

constantan thermocouple and controlled by an Air Products digital temperature indicator/controller. Although the thermocouple was not in direct contact with the sample, good thermal contact assured so that the sample temperature was the same as that of the cold stage. Before cooling of the sample, the sample chamber of the closed-cycle refrigerator was evacuated at room temperature.

Photolysis of *s*-P_2 was carried out in the closed-cycle refrigerator while the sample was held at a fixed temperature. In these experiments, the spectrofluorimeter light source was used as the photolysis source, typically at 310 nm, using an excitation monochromator slit width of 8 mm (14.4 nm bandwidth). Emission spectra were typically measured with an emission monochromator slit width of 1 mm (1.8 nm bandwidth). Fluorescence of photoproducts was excited with the spectrofluorimeter source lamp after photolysis, but at 310, 340, or 540 nm, depending upon the emission spectrum being investigated. Fluorescence spectra were typically recorded with the sample either having been recooled to ~12 K or at room temperature.

Triplet−triplet absorption spectra of *s*-P_2 in PMMA were determined in the diode array spectrophotometer. The sample film was masked with black photographic tape, sandwiched between the sapphire disks, and cooled in the closed-cycle refrigerator, as described above, to ~12 K. The cold tip of the refrigerator, containing the sample, was placed in the beam of the spectrophotometer, and spectra were taken in the 300 to 600 nm range. A frequency-doubled dye laser (CMX-4) firing at 30 Hz and ~325 nm for about 4 s provided excitation of the sample under computer control. The computer was programmed to take spectra before excitation, immediately after the laser pulse burst, and long after the burst. The triplet−triplet absorption spectrum was obtained by subtraction of "after" spectrum from the "immediate" spectrum, and the photoproduct spectrum was obtained by subtraction of the "before" spectrum from the "after" spectrum.

2.3. Crystal Structure Determination. Crystals for the diffraction study were grown by evaporation from solution in dichloromethane. As described above, freshly prepared, crystalline *s*-dipentacene oxidizes and adopts a brownish color. Several crystals were investigated before a suitably pure one was found. (As discussed below, the inclusion of solvent molecules in the *s*-dipentacene crystal, during the procedure used to grow crystals, may also hasten the subsequent decomposition process in these crystals.) The crystal finally selected was of tabular shape, approximately 500 × 150 × 150 microns. It was glued with a tiny drop of Devcon five-minute epoxy to a thin glass fiber mounted on a goniometer head.

Diffraction data were taken at beamline ×25 at the National Synchrotron Light source. The diffractometer was a hybrid comprised of a Nonius FAST diffractometer with a 200 mm square, four-module, CCD-based position-sensitive X-ray detector provided for the Brookhaven Biology Department by the group of W. Phillips of Brandeis University.[24] Because ×25 is a bright wiggler beamline, sufficient aluminum was placed in the beam to attenuate the beam by a factor of approximately four.

The wavelength of X-ray radiation used was 1.100(1) Å. The detector was placed 78.5 mm from the specimen and was tilted upward by 11° on the θ axis of the diffractometer to achieve 0.90 Å resolution at the edge of the detector. The crystal was rotated a full 360° in the X-ray beam: 120 five-second exposures, each of 3° rotation. The image data were reduced to structure factors with the HKL program suite.[25] Of the 3959 intensities measured and used in refinement, over one-quarter were measured four times, and over one-half were measured twice. The data were 87% complete at 0.9 Å resolution. The linear *R*-factor ($R = \sum|I - \langle I\rangle|/\sum I$) was 0.033 overall and 0.014 in the resolution range 1.22−0.90 Å.

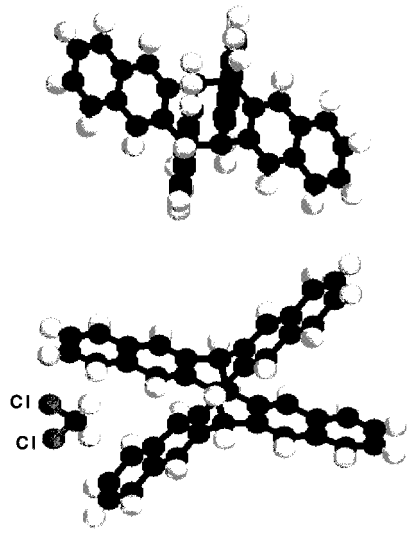

Figure 3. A ball-and-stick model of the unit cell showing two pentacene dimers, one of which is associated with a dichloromethane solvent molecule, the solvent used in the crystallization. The other dichloromethane molecule in the unit cell is associated with the same *s*-P_2 molecule and related to the one shown by the inversion symmetry of that molecule.

The structure was solved by direct methods[26] and refined by full-matrix least-squares analysis based on F. All hydrogen atoms were placed by geometrical considerations as fixed atoms in their ideal positions with temperature factors assumed from the attached carbon. The positions and anisotropic temperature factors were refined by full-matrix least-squares methods against $\Sigma(F_o - F_c)^2$, using the typical biweight weighting scheme. The final refinement cycle was based on 3859 reflections (43 low angle reflections were omitted by the biweight scheme,[27] presumably due to saturation effects of the detector). The 424 parameters varied gave a final conventional linear *R*-factor of 0.036 with weighted least-squares *R*-factor of 0.052. The final residual density map was essentially flat (max peak = 0.17e).

3. Results and Discussion

3.1. Structure Determination by X-ray Diffraction. The unit cell was refined by the HKL program SCALEPACK to be $a = 9.663$ Å, $b = 10.691$ Å, $c = 17.844$ Å, $\alpha = 67.675°$, $\beta = 72.743°$, and $\gamma = 71.618°$ in the space group $P\bar{1}$. The asymmetric unit of the $P\bar{1}$ unit cell is two halves of two independent molecules. Each molecule is completely centrosymmetric. Of the two molecules in the unit cell, one has dichloromethane molecules of solvation neatly tucked symmetrically into the wings on both sides of the dipentacene molecule. The other molecule does not have such solvent molecules in contact with it (See Figure 3).

Complete crystal structure information, in CIF format, is given in the Supporting Information for this paper. Because the synchrotron wavelength used in this structure determination was accurate to only about 0.1%, the bond lengths can be considered to be no more accurate than that. However, the precision within the relative scale factor given by a possible error in the wavelength is given in the table in the Supporting Information.

The mean bond lengths taken over all the examples of each bond in the structure are shown in Figure 4. The scatter among

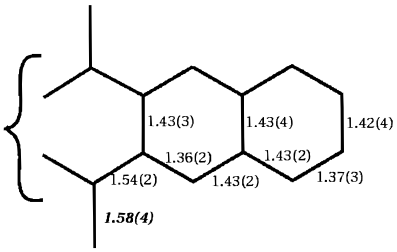

Figure 4. The mean bond lengths taken over all the examples of each bond in the structure.

the bond lengths of a given type is commensurate with the likely error in bond lengths arising from the precision of the data.

A surprising feature of the structure is that the two different molecules, one enclosing two dichloromethanes and one not, are so similar. Mean values of particular bond types are quite similar between the two different *s*-dipentacene molecules in the unit cell. In particular, the C−C single bonds that join the two halves of the *s*-dipentacene are both somewhat longer (1.58 Å) than a normal C−C single bond. Nevertheless, this distance is shorter than the ones observed in smaller aromatic dimers,[12−16] albeit the same as in these other dimers within our experimental error.

3.2. Spectroscopic Assignments. Figure 2a is an absorption spectrum of 1 mg of the photochemical reaction product dissolved in 1 mL of CH_2Cl_2. This product was separated on the basis of high solubility in CH_2Cl_2 and low solubility in ethyl ether, as described in section 2.1. The features can be tentatively identified by comparing them to absorption spectra of potential contaminants and related molecules in the same solvent: benzene, naphthalene, anthracene, and 1-chloronaphthalene. The dominant, sharp peak at 328 nm is similar to the lowest-energy absorption maximum arising from the transition to the S_1 excited state in naphthalene. Our determination of the crystal structure of the product confirms this assignment.

Using the molecular weight of dipentacene, 557 g mol^{-1}, we calculate a peak absorption (328 nm) cross section of 5.0×10^6 cm^2 mol^{-1}, or a molar extinction coefficient of 2200 l $mol^{-1}cm^{-1}$. This value is larger by a factor of ∼7X than the corresponding peak cross section of 2,3-dimethyl naphthalene in solution[28] but only about twice that of the value for the anthracene-tetracene photodimer.[29] Because *s*-dipentacene contains four naphthalene chromophores per molecule, its measured molar extinction coefficient is roughly consistent with these other determinations.

There are three other, smaller peaks in Figure 2b at 346, 364, and 384 nm. In different synthesis batches and at different stages of purification these peaks were generally observed in the same proportion to one another. Therefore, they are likely to originate from a single molecular species. These peaks in the absorption spectrum resemble a vibronic progression in the $S_1 \leftarrow S_0$ transition of anthracene in the same solvent, although shifted to longer wavelength by ∼5 nm. These results suggest that these peaks are due to dipentacene isomers of lower symmetry than *s*-P_2. Since the absorption cross section of anthracene is known to be larger than that of 2,3-dimethyl naphthalene by a factor of ∼30X,[28] the relatively weak peaks in Figure 2b probably represent a minor byproduct of the reaction.

One definitive behavior of pentacene dimers is its photodissociation reaction. When *s*-P_2 crystals or dimer-doped PMMA films are irradiated with ultraviolet wavelengths that overlap any part of the ultraviolet absorption edge, visible absorption bands, characteristic of the pentacene monomer, appear. This result is illustrated in Figure 5a with a dimer-doped film of

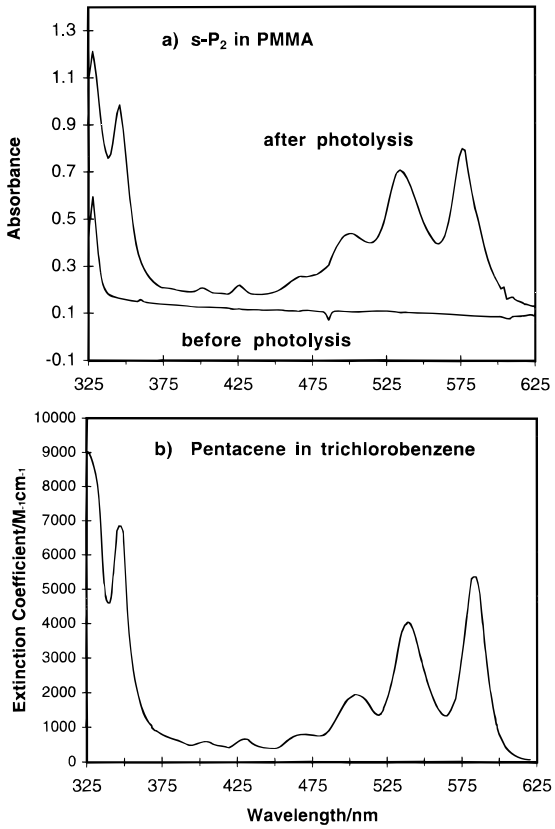

Figure 5. (a) Absorption spectrum of room-temperature photoproducts of *s*-P_2 in PMMA following near UV excitation with a low-pressure mercury lamp. (b) Absorption spectrum of pentacene in trichlorobenzene, replotted from ref 30.

PMMA at room temperature and pressure. The lower trace shows the absorption spectrum of clean *s*-dipentacene cast into a PMMA film at a concentration of ∼0.005 mol L^{-1}. Thirty minutes of broadband near-ultraviolet irradiation from a low-pressure mercury lamp yields the upper trace. The vibronic system between 450 and 600 nm is essentially identical to that of pentacene dissolved in trichlorobenzene[30] (Figure 5b) or dispersed directly in PMMA.[31] Pentacene can also be identified by its fluorescence spectrum, as we discuss in the following section.

The triplet−triplet absorption spectrum, shown in Figure 6, is quite similar to the one we obtained for the anthracene-tetracene photoadduct.[32] In turn, each of these triplet−triplet absorption spectra appears like line-broadened versions of the triplet−triplet absorption spectra of 2,3-dimethylnaphthalene.[32] This result provides additional confirmation of the identity of the *s*-dipentacene material.

3.3. Temperature-Dependent Photochemistry. The photodissociation shown in Figure 5a could be modified under low temperature and/or high-pressure conditions. We first consider the effect of low temperature. In Figures 7 through 9, the extent of reaction during irradiation and temperature cycling is followed by means of fluorescence spectra. When a dimer-doped PMMA film is excited with ultraviolet light, its dispersed emission is similar but not identical to that of dissolved naphthalene. The 310-nm photolysis of *s*-P_2 in PMMA at 13 K, monitored using its naphthalene-like emission spectrum ($\lambda = 325$ nm − 375 nm) vs irradiation time, in hours, is shown in Figure 7. Figure 7 documents the loss of *s*-P_2 as the sample is progressively photolyzed at a temperature of 13 K; after 22 h the *s*-P_2 in the sample is nearly depleted. At room temperature (not shown), the reaction is much more efficient: the same extent of dimer

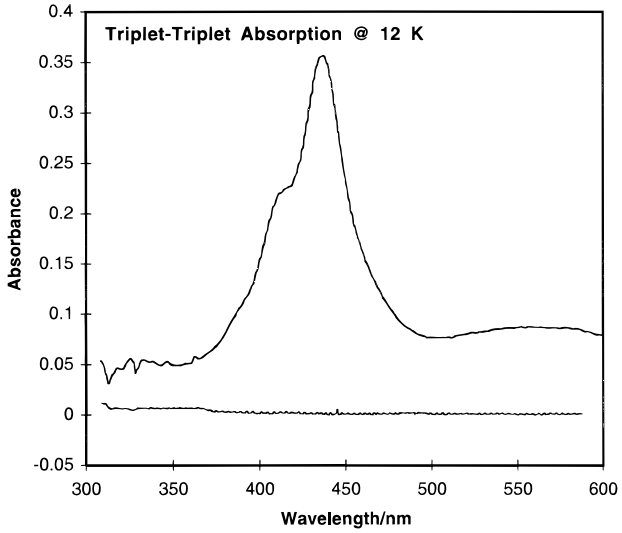

Figure 6. The triplet−triplet absorption spectrum of *s*-P_2 in PMMA at 12 K obtained immediately following laser excitation at 326 nm. The base line is the absorption spectrum obtained 15 s after excitation, showing an absence of triplet-state-induced, product-species absorption bands under the conditions of this experiment.

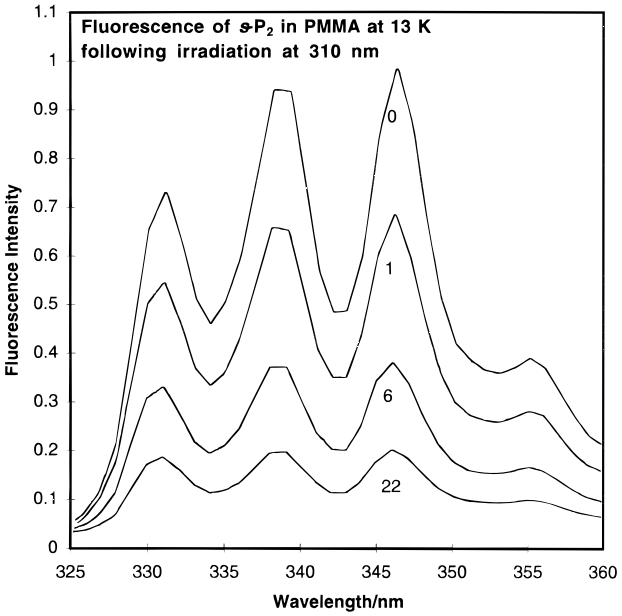

Figure 7. Fluorescence spectra of *s*-P_2 in PMMA at 13 K excited at 310 nm after different irradiation times at 310 nm, given in hours. The decrease in the naphthalenic absorption features monitors the photochemical decomposition of *s*-P_2.

depletion is reached after a mere 10 min of irradiation. When the 310 nm photolysis of *s*-P_2 is performed at room temperature, a prominent pentacene emission band grows in at the rate with which the naphthalenic emission band decreases.

While the dimer is being depleted by 310 nm photolysis at 13 K, there is a lack of any emission features that can be assigned to products. Figure 8 shows the spectral range in which pentacene monomers are expected: the 0−0 transition is found near 580 nm, with a vibronic maximum near 630 nm. Even after prolonged irradiation at 13 K, the emission, shown in the lower trace, is weak and unstructured. Following a temperature cycle up to room temperature (RT) and back to 13 K, however, the characteristic pentacene emission spectrum appears as shown in the upper trace. This and the previous observation suggest that a thermally unstable and spectroscopically undetected intermediate is trapped at 13 K. As will be discussed in later

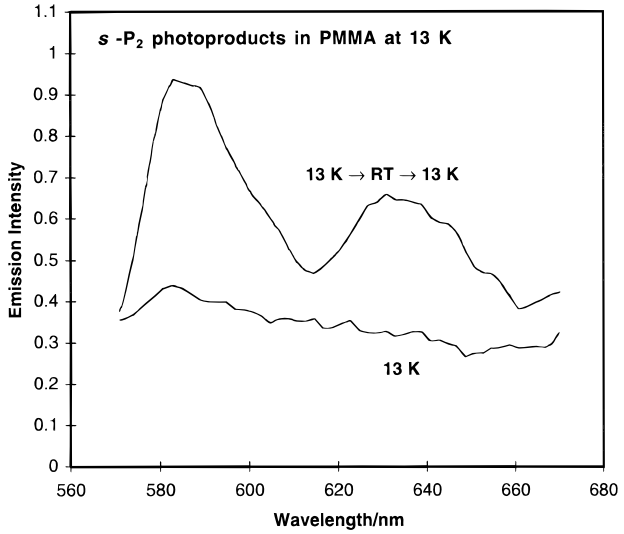

Figure 8. Emission spectra of *s*-P_2 in PMMA photoproducts at 13 K excited at 540 nm before and after cycling to room temperature. The lower curve is the emission from the sample after irradiation at 310 nm for 22 h, and the upper curve corresponds to the same sample after cycling to room temperature and recooling to 13 K.

sections, the "nonemissive" intermediate produced by irradiation at low temperature does not proceed further to the final pentacene product until the sample is cycled to higher temperature.

Although we do not have direct structural information about the nonemissive photoproduct of the dimer, assuming that this photochemistry is analogous to that of ditetracene,[11] then it is reasonable to assign the nonemissive intermediate as a "broken dimer". The lowest energy excited state of this dimer pair presumably lies well to the red of this spectral region. Thus, emission from this broken dimer, if any, may occur in the infrared in a region not accessible to our detection methods.

The temperature-dependent photochemical yield of *s*-P_2 was obtained by photolyzing at various temperatures for a fixed amount of time, after which the samples were raised to room temperature. Figure 9 shows the pentacene photoproduct emission spectra, measured at room temperature, after 60 min of irradiation at the indicated temperatures. Note that after photoexcitation at low temperature, all spectra were obtained at room temperature to ensure that all nonemissive photochemical intermediates, e.g., broken dimers, were allowed to proceed to the final pentacene product. An analysis of the integrated spectral intensity quantifies the reduced photochemical yield of pentacene when excited at lower temperatures. A plot of the logarithm of the relative intensity of these spectra versus inverse temperature yields an activation energy for production of the photochemical product, as shown in Figure 10. There is a small, temperature-independent contribution to the photochemical yield that dominates at temperatures below 75 K. The temperature-dependent quantum yield of pentacene from *s*-P_2, obtained from Figures 9 and 10, yields an activation energy of 3.5 kJ M^{-1}. This activation energy is similar to the one previously observed for breaking of the related dimer of anthracene in PMMA,[23] but it is significantly smaller than the value reported for the anthracene-tetracene photoadduct in an organic solvent.[29] Differences in the host/solvent conditions likely are responsible for the large differences in these activation energies.

On the basis of our previous studies[23,32] and those of others[29] on related polyacene photodimers, we speculate that the

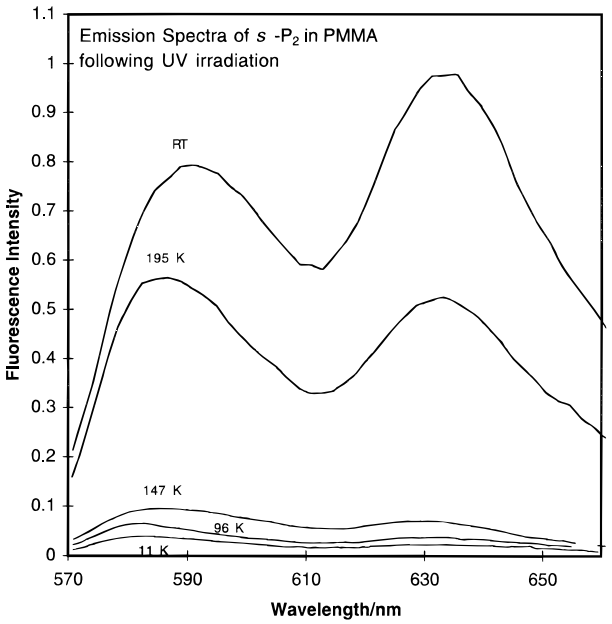

Figure 9. Emission spectra of *s*-P_2 in PMMA photoproducts after 60 min of irradiation at 310 nm at the indicated temperatures. The spectra were all measured at room temperature.

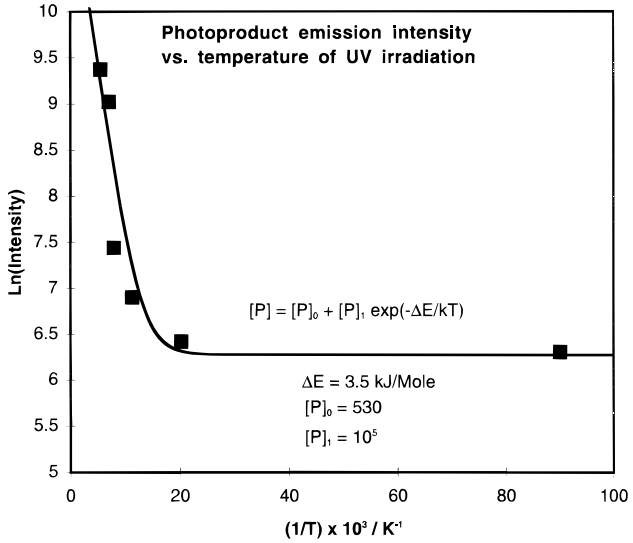

Figure 10. The photoproduct emission intensity at 585 nm, obtained from Figure 9, vs T^{-1}. The curve is an Arrhenius fit to the data yielding an activation energy of 3.5 kJ mol^{-1}.

"activation energy" for the photochemical production of pentacene from *s*-P_2 is likely due to a complicated process that may involve multiphoton excitation above the lowest triplet state of the molecule and that it also may require thermal energy of the polymer matrix. The only information we have concerning the triplet state of P_2 is the T−T absorption spectrum (Figure 6), and it is quite similar to that of the anthracene−tetracene photoadduct.[32] The inhibition of the photochemistry at low temperature might be due to a back reaction to reform *s*-P_2 when the lattice does not permit sufficient rearrangement of the two pentacene monomer product molecules. When the two pentacene monomers are held in close proximity after photoexcitation the barriers for reformation of the *s*-P_2 molecule are expected to be lower, resulting in a lower yield of pentacene monomer product, as shown in Figure 9. In addition, much of the chemistry that does occur at low-temperature results in the formation of a trapped, nonemissive, broken dimer that does not convert to pentacene product until the temperature is raised. This was illustrated in Figure 8.

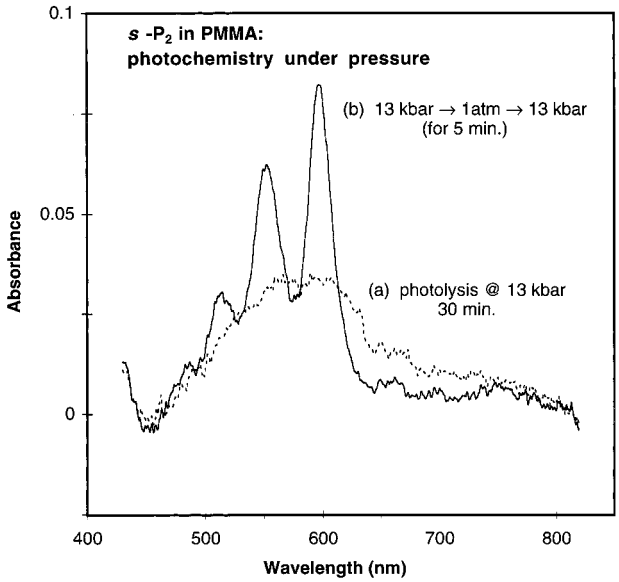

Figure 11. Absorption spectra (a) following photolysis of *s*-dipentacene at 340 nm, at ∼13 kbar and 300 K (dotted curve) and (b) the appearance of the pentacene monomer spectrum following a subsequent 5 min pressure release to 0 kbar and compression back to 13 kbar (solid curve).

It should be noted that there are spectral differences in the pentacene product emission spectrum, taken at room temperature, when the photochemistry is performed at different temperatures, as shown in Figure 9. Specifically, the relative magnitude of the higher energy vibronic band at 590 nm is enhanced relative to the lower energy band at 633 nm when the photochemistry is performed at lower temperatures. One can speculate that at low temperatures the photochemistry that occurs, albeit at a reduced rate, effectively selects *s*-P_2 molecules that are situated in the matrix such that pentacene monomer products have sufficient mobility to separate. This subset of matrix environments of the *s*-P_2 molecules could also lead to unique Franck−Condon factors for the product pentacene molecules, relative to the more common matrix environments that can only lead to photochemistry at higher temperatures.

3.4. Photochemistry under Pressure. At high pressure, i.e., 13 kbar, ultraviolet excitation of *s*-dipentacene in PMMA yields photochemical "broken dimer" species that are stable at room temperature. The high pressure trapped "broken dimer" in PMMA displays a broad and featureless absorption spectrum, as shown in Figure 11. The pressure-trapped "broken dimer" may be similar to the trapped broken-dimer observed under low temperature conditions. Upon pressure release, the broad and featureless absorption spectrum of the high pressure "broken dimer" spontaneously yields a sharpened absorption spectrum characteristic of monomeric pentacene in PMMA, as shown in Figure 11. In these experiments, to adjust for the large pressure shift of the pentacene absorption spectrum the sample was repressurized to 13 kbar for all spectra. Thus, the monomeric spectrum following pressure release (and return to high pressure) is seen to sharpen significantly and blueshift slightly relative to the "broken dimer" spectrum. This behavior is reminiscent of the low-temperature results that we previously obtained for "broken dimers" of tetracene from ditetracene following a temperature cycle to room temperature.[11] Thus, we conclude that these "broken dimers" of pentacene also do not have parallel transition moments and are not "sandwich dimers."

The increased density and/or decreased molecular diffusion in PMMA at high pressure appears to restrict the molecular

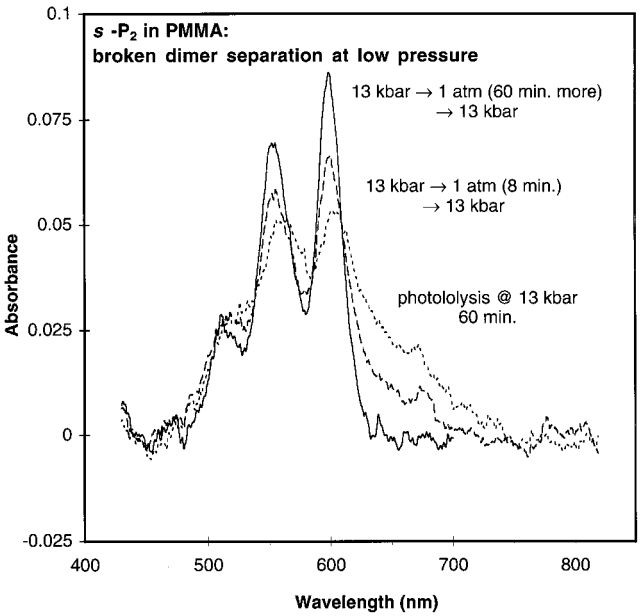

Figure 12. Absorption spectra monitoring the photolysis of *s*-dipentacene at 340 nm, at ~13 kbar, and 300 K (dotted curve), followed by pressure release periods of 8 min (dashed curve) and 8 min + 60 min (solid curve), followed by compression back to 13 kbar.

motion needed for the "broken dimer" to break apart into two pentacene monomers. Upon the release of pressure, the "broken dimer" is observed to proceed spontaneously to pentacene monomer product. In addition, multiple pressure cycling experiments have also characterized the ability of pressure to control the amount of conversion of the "broken dimer" into pentacene monomer product (see below).

The total pentacene yield generated by photoexcitation of *s*-P_2 in PMMA at high pressure followed by pressure release, although not quantified, was significantly less than for similar photoexcitation of a sample at ambient pressure. The reduced photochemical reactivity at high pressure is attributed to an increased back reaction to reform *s*-P_2 due to the shorter intermolecular distances at high pressure.

No red shifted emission has been observed for the trapped broken dimer following photochemical excitation of *s*-P_2. The intermediate "broken dimer" did not show any detectable red-shifted emission either at low temperature nor at high pressure. These results are in contrast to the photochemistry of dianthracene[23] and the ditetracenes[11] in which red-shifted emission was observed for the trapped broken dimers at low temperature.

The rate at which the high-pressure broken dimer converts to pentacene products depends on the total time spent at low pressure, as shown in Figure 12. Pressure cycling experiments in which the pressure is cycled from high to low-pressure several times show that high pressure can be used to control the amount of conversion of the "broken-dimer" intermediate to pentacene monomer product. The ability to stop the dissociation of the broken dimer by pressurization also permits an estimation of the kinetics for conversion of the broken dimer to pentacene monomers at ambient pressure.

The kinetics of the "broken dimer" conversion to pentacene monomers at ambient pressure was estimated by the decay of the broad "broken-dimer" absorption wing near 650 nm versus total time at low pressure. Since only the "broken dimer" has significant absorbance at 650 nm, the absorbance decay measures the decreasing "broken-dimer" concentration, yielding a ~15 min time constant (see Figure 12).

4. Conclusions

The following observations and conclusions have been obtained: (1) The first reported photochemical synthesis of the symmetric addition product dimer of pentacene (*s*-dipentacene) from a room-temperature solution of pentacene. (2) X-ray crystal structure determination of the *s*-P_2 product confirmed the symmetric product and yielded the structure and bond lengths of the s−P_2 product species. The X-ray results yield a triclinic, $P\bar{1}$ crystal symmetry and also showed that the crystals grown from a dichloromethane solution incorporated two solvent molecules per unit cell. (3) Spectroscopic measurements have been used to characterize the UV photochemistry of *s*-P_2 in PMMA films to produce "broken-dimers" which can subsequently fall apart to yield spectroscopically identifiable pentacene monomers. (4) Spectroscopic studies of the UV photochemistry of *s*-P_2 doped PMMA at low temperature showed that *s*-P_2 was being removed (Figure 7), but no pentacene monomer absorption or emission was detected (Figure 8). This low-temperature product was identified as a "broken-dimer". (5) By raising the temperature, a "broken-dimer" formed at low temperature was observed to separate into spectroscopically identifiable pentacene monomers (Figure 8). (6) The photochemical decomposition of the naphthalenic chromophores of *s*-P_2 occurs at a reduced rate at low temperature (Figure 9 and 10), and yields an activation energy of 3.5 kJ M^{-1}. The reduced photochemical rate at low temperature is attributed to an increased back reaction to reform *s*-P_2 at low temperature. (7) The UV photochemistry of *s*-P_2 doped PMMA at high pressure (13 kbar) also did not yield a pentacene monomer product spectrum (Figure 11). The high-pressure product is attributed to a trapped "broken dimer", analogous to that formed at low temperature. (8) A reduced photochemical yield at high pressure was observed and attributed to an increased back reaction to reform *s*-P_2 under compression. (9) At low pressure the "broken-dimers" formed at high pressure separate to yield spectroscopically identifiable pentacene monomers (Figure 11). This separation process occurs on a time scale of ~15 min at low pressure (Figure 12).

One striking observation of this study is the analogous way in which both low temperature and high-pressure affect the UV photochemistry of *s*-P_2 in PMMA. Specifically: (1) inhibition of the UV photochemical decomposition of *s*-P_2 in PMMA at either low temperature or high pressure, (2) trapping of the photoproducts at low temperature or high pressure in a non-emissive, "broken-dimer" species, and (3) transformation of the trapped "broken-dimer" species into spectroscopically identifiable pentacene product by either warming or pressure release. These effects undoubtedly arise from the fact that low-frequency vibrations of the lattice have smaller amplitudes under conditions of both low temperature and high pressure.

Acknowledgment. E.L.C. acknowledges support from a National Science Foundation grant (Grant CHE-9714886). G.W.S. acknowledges support from the UCR Committee on Research. X-ray diffraction measurements at beamline X25 at the Brookhaven National Laboratory National Synchrotron Light Source were funded by the Offices of Basic Energy Science and of Biological and Environmental Research of the U.S. Department of Energy, and by the National Science Foundation. Two of us (E.L.C. and G.W.S.) wish to acknowledge the many contributions to our professional lives and the scientific stimulation made by our dear friend and colleague, Professor Bryan E. Kohler. It is to his memory that this paper is dedicated.

Supporting Information Available: Tables of crystallographic structure data for *s*-dipentacene. Supporting Information is available free of charge via the Internet at http://pubs.acs.org.

References and Notes

(1) Frizsche, J. *J. Prakt. Chem.* **1866**, *101*, 337.
(2) Linebarger, C. *Am. Chem. J.* **1892**, *14*, 597.
(3) Coulson, C. A.; Orgel, L. E.; Taylor, W.; Weiss, J. *J. Chem. Soc.* **1955**, 2961.
(4) Wei, K. S.; Livingston, R. *Photochem. Photobiol.* **1967**, *6*, 229.
(5) Lapouyade, R.; Normande, A.; Bouas-Laurent, H. *Tetrahedron* **1980**, *36*, 2311.
(6) Bouas-Laurent, H.; Castellan, A. *Chem. Commun.* **1970**, 1648.
(7) Hellner, C.; Lindqvist, L.; Roberge, P. C. *Trans. Faraday Soc. 2* **1972**, *68*,1928.
(8) Birks, J. B.; Appleyard, J. H.; Pope, R. *Photochem. Photobiol.* **1963**, *2*, 493.
(9) Tomlinson, W. J.; Chandross, E. A.; Fork, R. L.; Pryde, C. A.; Lamola, A. A. *Appl. Opt.* **1972**, *11*, 533.
(10) Chandross, E. A.; Ferguson, J.; McCrae, E. G. *J. Chem. Phys.* **1966**, *45*, 3546. Ferguson, J.; Mau, A. W−H. *Mol. Phys.* **1977**, *27*, 377. Ferguson, J.; Mau, A. W−H.; Morris, J. M. *Austr. J. Chem.* **1991**, *91*, 26.
(11) Iannone, M. A.; Scott, G. W. *Chem. Phys. Lett.* **1990**, *171*, 569.
(12) Ehrenberg, M. *Acta Crystallogr.* **1966**, *20*, 177.
(13) Gaultier, J.; Hauw, C.; Desvergne, J. P.; Lapouyade, R. *Cryst. Struct. Commun.* **1975**, *4*, 497.
(14) Ferguson, J.; Mau, A. W−H.; Whimp, P. O. *J. Am. Chem. Soc.* **1979**, *101*, 2363.
(15) Sinha, H. K.; Lough, A. J.; Yates, K. *J. Org. Chem.* **1991**, *56*, 3727.
(16) Battersby, T. R.; Gantzel, P.; Baldridge, K. K.; Siegel, J. S. *Tetrahedron Lett.* **1995**, *36*, 845.
(17) Ferguson, J. *Chem. Rev.* **1986**, *86*, 957.
(18) Bouas-Laurent, H.; Desvergne, J.-P. Cycloaddition reactions involving 4*n* electrons: (4+4) cycloaddition reactions between unsaturated conjugated systems. In *Photochromism Molecules and Systems*; Dürr, H., Bouas-Laurent, H., Eds.; Elsevier: Amsterdam, 1990; Chapter 14, pp 561−630.
(19) Salt, K.; Scott, G. W. *J. Phys. Chem.* **1994**, *98*, 9986.
(20) Iannone, M. A.; Mackay, R. A.; Scott, G. W.; Yamashita, T. *Proc. Photo-Opt. Instrum. Eng.* **1990**, *1213*, 155.
(21) Berg, O.; Chronister, E. L. *J. Chem. Phys.* **1997**, *106*, 4401.
(22) Iannone, M. A.; Salt, K. L.; Scott, G. W.; Yamashita, T. *Proc. Photo-Opt. Instrum. Eng.* **1991**, *1559*, 172.
(23) Iannone, M. A.; Scott, G. W. *Mol. Cryst. Liq. Cryst.* **1992**, *211*, 375.
(24) Phillips, W. C.; Stanton, M.; Hua, Q.; Stewart, A.; O'Mara, D.; Sweet, R. M. 1998. Manuscript in preparation.
(25) Otwinowski Z.; Minor, W. Processing of X-ray diffraction data collected in oscillation mode. In *Methods in Enzymology, Macromolecular Crystallography, Part A*; Carter, C. W., Jr., Sweet, R. M., Eds.; Academic Press: San Diego, 1998; Vol. 276, Chapter 20, pp 307−326.
(26) Sheldrick, G. M. *SHELX97;* University of Gottingen: Germany, 1997.
(27) Prince, E.; Nicholson, W. L. *Acta Crystallogr.* **1983**, *A39*, 407.
(28) Berlman, I. B. *Handbook of Fluorescence Spectra of Aromatic Molecules*, 2nd ed.; Academic: New York, 1971.
(29) Yamamoto, S.; Grellmann, K.-H. *Chem. Phys. Lett.* **1982**, *92*, 533.
(30) Clar, E. *Polycyclic Hydrocarbons*; Academic: London, 1964; p 425.
(31) Molenkamp, L. W.; Wiersma,D. A *J. Chem. Phys.* **1984**, *80*, 3054.
(32) Iannone, M. A.; Scott, G. W. *J. Phys. Chem.* **1991**, *95*, 3206.